Journal of Biomolecular NMR, **24:** 133–142, 2002.
KLUWER/ESCOM

Observation of H-bond mediated $^{3h}J_{H2H3}$ coupling constants across Watson–Crick AU base pairs in RNA

Burkhard Luy[a,*], Uwe Richter[a,**], Eric S. DeJong[a], Ole W. Sørensen[b] & John P. Marino[a,***]
[a]*Center for Advanced Research in Biotechnology of the University of Maryland Biotechnology Institute and the National Institute of Standards and Technology, 9600 Gudelsky Dr., Rockville, MD 20850, U.S.A.;* [b]*Department of Chemistry, Carlsberg Laboratory, Gamle Carlsberg Vej 10, DK 2500 Valby, Denmark*

Received 2 July 2002; Accepted 28 August 2002

Key words: $^{3h}J_{HH}$ coupling constant, E. COSY, hydrogen bond, RNA

Abstract

$^{3h}J_{H2H3}$ trans-hydrogen bond scalar coupling constants have been observed for the first time in Watson-Crick AU base pairs in uniformly ^{15}N-labeled RNA oligonucleotides using a new $^{2h}J_{NN}$-HNN-E. COSY experiment. The experiment utilizes adenosine H2 (AH2) for original polarization and detection, while employing $^{2h}J_{NN}$ couplings for coherence transfer across the hydrogen bonds (H-bonds). The H3 protons of uracil bases are unperturbed throughout the experiment so that these protons appear as passive spins in E. COSY patterns. $^{3h}J_{H2H3}$ coupling constants can therefore be accurately measured in the acquisition dimension from the displacement of the E. COSY multiplet components, which are separated by the relatively large $^{1}J_{H3N3}$ coupling constants in the indirect dimension of the two-dimensional experiment. The $^{3h}J_{H2H3}$ scalar coupling constants determined for AU base pairs in the two RNA hairpins examined here have been found to be positive and range in magnitude up to 1.8 Hz. Using a molecular fragment representation of an AU base pair, density functional theory/finite field perturbation theory (DFT/FPT) methods have been applied to attempt to predict the relative contributions of H-bond length and angular geometry to the magnitude of $^{3h}J_{H2H3}$ coupling constants. Although the DFT/FPT calculations did not reproduce the full range of magnitude observed experimentally for the $^{3h}J_{H2H3}$ coupling constants, the calculations do predict the correct sign and general trends in variation in size of these coupling constants. The calculations suggest that the magnitude of the coupling constants depends largely on H-bond length, but can also vary with differences in base pair geometry. The dependency of the $^{3h}J_{H2H3}$ coupling constant on H-bond strength and geometry makes it a new probe for defining base pairs in NMR studies of nucleic acids.

Introduction

Hydrogen bonds (H-bonds) play a key role in both the stability and specificity of secondary and tertiary folding interactions in nucleic acids. The ability to directly observe individual hydrogen bonds and identify the participating atoms can provide valuable information about macromolecular structure and strength of interatomic interactions (for recent reviews see Dingley et al., 2001; Gemmecker, 2000; Grzesiek et al., 2001; Majumdar and Patel, 2002). In addition to providing a physical measure for the strength of H-bonds, trans-hydrogen bond scalar correlations can also yield unambiguous assignment for H-bond coupled nuclei. As a result, trans-hydrogen bond coupling constants can provide both unique nuclear magnetic resonance (NMR) restraints for defining structure and novel assignment pathways. Direct physical evidence for the existence of H-bonds was first established through the measurement of trans-hydrogen bond $^{2h}J_{NN}$ scalar couplings in nucleic acids (Dingley and Grzesiek, 1998; Pervushin et al., 1998). Following these seminal

Current addresses: *Institut für Organische Chemie und Biochemie II, TU München, Lichtenberg-Str. 4, D-85747 Garching, Germany; **Forschungsinstitut für Molekulare Pharmakologie, Robert-Rössle-Str. 10, D-13125 Berlin, Germany.
***To whom correspondence should be addressed. E-mail: marino@carb.nist.gov

studies, a number of methods have been used to measure additional trans-hydrogen bond associated scalar couplings in both nucleic acids (Dingley et al., 1999, 2000; Wohnert et al., 1999; Hennig and Williamson, 2000; Liu et al., 2000; Luy and Marino, 2000; Majumdar et al., 1999, 2001a,b; Pervushin et al., 2000) and proteins (Cordier and Grzesiek, 1999; Cordier et al., 1999; Cornilescu et al., 1999a,b; Wang et al., 1999; Liu et al., 2000; Pietrzak et al., 2001; Meissner and Sørensen, 2000a,b).

In nucleic acids, relatively large $^{2h}J_{NN}$ coupling constants ($^{2h}J_{NN} \sim$ 6–10 Hz) have been observed between imino nitrogens and their corresponding ^{15}N partners in hydrogen bonding interactions in base pairs, triplets and quadruplexes (Dingley and Grzesiek, 1998; Pervushin et al., 1998; Wohnert et al., 1999; Dingley et al., 1999, 2000; Hennig and Williamson, 2000; Liu et al., 2000; Luy and Marino, 2000; Majumdar et al., 1999a, 2001a,b). Smaller $^{1h}J_{HN}$ coupling constants ($^{1h}J_{HN} \sim$ 2–4 Hz) have also been measured between the imino proton and H-bond acceptor nitrogen (Dingley et al., 1999; Pervushin et al., 1998). The magnitude of these $^{2h}J_{NN}$ and $^{1h}J_{HN}$ scalar coupling constants has been shown to correlate well with H-bond length, $^{1}J_{NH}$ coupling constants and the imino proton and nitrogen chemical shifts (Dingley et al., 1999; Scheurer and Bruschweiler, 1999; Barfield et al., 2001). Three and four bond $^{nh}J_{NN}$ and $^{nh}J_{NC}$ coupling constants (e.g., $^{4h}J_{NN} \sim$ 0.14 Hz and $^{3h}J_{NC} \sim$ 0.2 Hz) associated with hydrogen bonds in nucleic acids (Dingley et al., 2000; Majumdar et al., 2001) and two and three bond $^{nh}J_{HC'}$, $^{nh}J_{HC\alpha}$ and $^{nh}J_{NC'}$ coupling constants (e.g., $^{2h}J_{HC'}$ and $^{3h}J_{NC} \sim$ 0.5 Hz) associated with hydrogen bonds in proteins (Cordier and Grzesiek, 1999; Cornilescu et al., 1999a; Liu et al., 2000; Meissner and Sørensen, 2000a,b) have also been measured and used to characterize H-bond interactions. In addition, weak phosphorus-proton and phosphorus-nitrogen coupling constants ($^{3h}J_{NP}$ and $^{2h}J_{HP}$ ranging from 0.2 to 4.6 Hz) have been measured between nucleotide cofactors and proteins (Lohr et al., 2000; Mishima et al., 2000) and trans-hydrogen bond coupling constants have even been observed in instances when the H-bond mediating proton resonance is severely exchange broadened (Hennig and Geierstanger, 1999; Majumdar et al., 1999b; Hennig and Williamson, 2000; Luy and Marino, 2000).

Several theoretical studies have also been carried out using model atomic systems to investigate the structural dependency of the magnitude and sign of *J*-coupling constants, as well as magnetic shielding, associated with hydrogen bonding (Dingley et al., 1999; Scheurer and Bruschweiler, 1999; Arnold and Oldfield, 2000; Barfield et al., 2001; Barfield, 2002; Benedict et al., 2000; Bryce and Wasylishen, 2001; Czernek et al., 2000; Czernek and Bruschweiler, 2001; Del Bene and Bartlett, 2000; Del Bene and Jordan, 2001; Del Bene et al., 2001; Dunger et al., 2000; Guerra et al., 2000; Pecul et al., 2000; Wilkens et al., 2002). In general, calculations using density function theory (DFT) and finite field perturbation theory (FPT) have been found to closely reproduce the size and trends observed experimentally for trans-hydrogen bond coupling constants.

In this study, $^{3h}J_{H2H3}$ trans-hydrogen bond scalar coupling constants between the adenosine H2 (AH2) proton and the uracil H3 proton in AU base-pairs are observed for the first time in two uniformly ^{15}N-labeled RNA hairpins using a new $^{2h}J_{NN}$-HNN-E. COSY experiment. $^{3h}J_{H2H3}$ coupling constants measured for AU pairs in these two RNA hairpins have been found to be positive and vary in magnitude between 0.1 and 1.8 Hz. DFT/FPT calculations carried out to assess the dependence of $^{3h}J_{H2H3}$ coupling constant on hydrogen bond distance and AU base pair geometry indicate that the size of these coupling constants depend mainly on H-bond length, but can also vary with differences in base pair geometry. Although the trends determined by the theoretical calculations are found to agree qualitatively with the observed experimental data, the calculations did not reproduce the full magnitude range of the observed $^{3h}J_{H2H3}$ coupling constants and so are used only for making relative comparisons.

Materials and methods*

Sample preparation

Uniformly ^{15}N-enriched forms of two RNA hairpins, a 23mer DIS23-AG, derived from the dimerization initiation site (DIS) of HIV-1 (Paillart et al., 1996), and a 29mer CopA29, derived from the R1 plasmid replication control system (Wagner and Simons, 1994), were prepared by *in vitro* T7 polymerase run-off transcription using synthetic DNA oligonucleotide templates

*Certain commercial equipment, instruments, and materials are identified in this paper in order to specify the experimental procedure. Such identification does not imply recommendation or endorsement by the National Institute of Standards and Technology, nor does it imply that the material or equipment identified is necessarily the best available for the purpose.

according to the method of Milligan and Uhlenbeck (Milligan and Uhlenbeck, 1989). Synthetic DNA templates used in T7 polymerase run-off transcriptions were prepared in-house and purified using denaturing polyacrylamide gel electrophoresis (PAGE). Unlabeled nucleotides used in the T7 polymerase run-off transcriptions were purchased from Pharmacia and ^{15}N-labeled nucleotides were prepared enzymatically from *E. coli* biomass according to previously published methods (Batey et al., 1992; Nikonowicz et al., 1992). RNA samples were desalted by dialysis against DEPC treated ddH_2O, then extensively dialyzed against standard NMR buffer (25 mM NaCl, 1 mM Cacodylate [pH 6.5]), lyophilized to dryness and resuspended in 90% H_2O/10% D_2O to a final volume of $\sim$250 µl in Shigemi limited volume NMR tubes (Shigemi, Inc., Allison, PA). NMR sample concentrations ranged from 1.0 to 1.5 mM.

NMR spectroscopy

$^{2h}J_{NN}$-HNN-E. COSY spectra were recorded at 298 K on a Bruker AVANCE 600 MHz spectrometer (Bruker Instruments, Billerica, MA) equipped with a triple-resonance ^{1}H, ^{13}C, ^{15}N triple-axis gradient probe and linear amplifiers on all three channels. Other specific experimental delays and parameters are given in the Figure captions. Spectra were collected on the DIS23-AG sample using sweep widths of 14 000 Hz in ω_2 and 7000 Hz in ω_1, 2 K by 128 complex data points in t_2 and t_1, respectively, (t_{1max} = 18.3 ms and t_{2max} = 146.3 ms) and 192 scans per increment. Spectra were collected on the CopA29 sample using sweep widths of 5400 Hz in ω_2 and 7000 Hz in ω_1, 2 K by 128 complex data points in t_2 and t_1, respectively, (t_{1max} = 18.3 ms and t_{2max} = 379.2 ms) and 256 scans per increment. All spectra were processed and analyzed on a Silicon Graphics UNIX workstation using the XWINNMR software package (Bruker Instruments, Billerica, MA). Spectra were apodized in the acquisition dimension using a 90° shifted sine-bell shaped window function over 512 complex points and zero-filled to achieve a resolution of $\sim$0.22 Hz/pt. $^{3h}J_{H2H3}$ coupling constants were measured by first summing the rows through each of the two multiplet components of the E. COSY cross peak and then measuring the frequency displacement between the two traces as previously described (Griesinger et al., 1985, 1986, 1987). This fitting approach bypasses the need to know anything about peak shapes and allowed accurate determination of the $^{3h}J_{H2H3}$ coupling constants.

DFT/FPT calculations

The dependence of the $^{3h}J_{H2H3}$ coupling constants on H-bond distance and geometry was calculated with the GAUSSIAN98* package. The model system representing the hydrogen bonding region of the AU base pair was constructed with ideal coordinate geometry using the biopolymer module of the program Insight II (Accelrys Inc., CA) and systematic structure variations were carried out using MOLDEN (Schaftenaar and Noordik, 2000). The positions of the hydrogen atoms added with MOLDEN were relaxed at the B3LYP/6-31G** level of theory while keeping the rest of the system at the experimental geometry. Some initial calculations were also performed using the full AU base pair and the size of the resulting *J*-coupling constants were found to be practically identical to those extracted from calculations with the AU fragment. As a result, the calculations described here were all carried out with the AU model fragment since this dramatically reduced the time required for computational calculations.

For the calculation of the Fermi contact contribution to the *J*-coupling constant, the unrestricted DFT formalism was employed in combination with the FIELD option in GAUSSIAN, which allows the introduction of a spin perturbation at a specific atom (Onak et al., 1999). These finite perturbation theory (FPT) methods, originally developed by Pople et al. (Pople et al., 1968), result in non-zero spin densities in formally closed-shell systems, from which the Fermi contact terms can be extracted. The Fermi contact contributions were calculated at the UB3LYP/6-311G** level of theory on a complete 3-dimensional grid of 210 points on the potential surface, varying the N-N distance (range: 270 to 310 pm, step size: 10 pm),

*Gaussian 98 (Revision A.10), M.J. Frisch, G.W. Trucks, H.B. Schlegel, G.E. Scuseria, M.A. Robb, J.R. Cheeseman, V.G. Zakrzewski, J.A. Montgomery, Jr., R.E. Stratmann, J.C. Burant, S. Dapprich, J.M. Millam, A.D. Daniels, K.N. Kudin, M.C. Strain, O. Farkas, J. Tomasi, V. Barone, M. Cossi, R. Cammi, B. Mennucci, C. Pomelli, C. Adamo, S. Clifford, J. Ochterski, G. A. Petersson, P.Y. Ayala, Q. Cui, K. Morokuma, D.K. Malick, A.D. Rabuck, K. Raghavachari, J.B. Foresman, J. Cioslowski, J.V. Ortiz, A.G. Baboul, B.B. Stefanov, G. Liu, A. Liashenko, P. Piskorz, I. Komaromi, R. Gomperts, R.L. Martin, D.J. Fox, T. Keith, M.A. Al-Laham, C.Y. Peng, A. Nanayakkara, C. Gonzalez, M. Challacombe, P.M.W. Gill, B.G. Johnson, W. Chen, M.W. Wong, J.L. Andres, M. Head-Gordon, E.S. Replogle and J.A. Pople, Gaussian, Inc., Pittsburgh PA, 1998.

the N-H distance (range: 95 to 120 pm, step size: 5 pm), and the planar angle ζ as defined in Figure 4A (range: 100° to 130°, step size: 5°). In addition, Fermi contact contributions were calculated by leaving the H-bond distance fixed to the ideal length and varying the angle ϕ or the base pair propeller twist as defined in Figure 4A (range: −45° to 25°, step size: 10°) and the dihedral angle θ spanned by H2-C2-N1···H3 as defined in Figure 4A (range: −50° to 50°, step size 10°). Since other contributions to the *J*-coupling constant have been shown to be much smaller and less dependent on structural variation, only the Fermi contact interaction was considered in the calculations (Geertsen et al., 1987; Malkin et al., 1994; Malkina et al., 1996).

Results and discussion

The $^{2h}J_{NN}$-HNN-E. COSY experiment used to measure $^{3h}J_{H2H3}$ scalar coupling constants in AU base-pairs in uniformly ^{15}N-labeled RNA is shown in Figure 1. The experiment is adapted from the previously described $^{2h}J_{NN}$-HNN-COSY experiment (Hennig and Geierstanger, 1999; Hennig and Williamson, 2000; Luy and Marino, 2000). It utilizes adenosine H2 (AH2) for original polarization and detection by adjusting the initial and final proton-nitrogen INEPT delays to optimally transfer adenosine H2 → N1 magnetization [$^2J_{NH} \sim -15$ Hz coupling; $\Delta = 0.5(^1J_{NH})$]. $^{2h}J_{NN}$ couplings are employed for coherence transfer across the N1···H3-N3 hydrogen bond and allow for direct correlation of the adenosine H2 proton with the uracil N3 H-bond donor nitrogen (Figure 2A). Adenosine H2 protons detected in the experiment are normally well resolved and exhibit favorable relaxation properties, which compensates for the lower transfer efficiency encumbered by using this two-bond $^2J_{HN}$ magnetization transfer pathway. The E. COSY (Griesinger et al., 1985, 1986, 1987) cross peak from which the $^{3h}J_{H2H3}$ coupling constants are measured (Figure 2B) is generated by evolving N3 nitrogen resonances in the indirect t_1 dimension of the two-dimensional $^{2h}J_{NN}$-HNN-E. COSY experiment without proton decoupling and then using a selective 90° proton G4-pulse (Emsley and Bodenhausen, 1989) in the reverse INEPT to leave the spin state of the uracil H3 proton unperturbed during the N1 → H2 back-transfer of magnetization. In the resulting spectrum, the H3 protons of uracil appear as passive spins in E. COSY patterns. The $^{3h}J_{H2H3}$ coupling constants can therefore be accurately measured in the acquisition dimension from the displacement of the E. COSY cross peak multiplet components which are separated by the relatively large $^1J_{H3N3}$ coupling constants in the indirect dimension of the two-dimensional experiment. In the $^{2h}J_{NN}$-HNN-E. COSY experiment, fast exchange of the passive H3 imino proton resonance with solvent can result in the possibility of self-decoupling and a scaling down of the observed couplings constants. For the case of a first order effect of solvent exchange, observation of significantly broadened and unresolved components for the E. COSY cross peaks would be expected. In the present applications, the components of the E. COSY cross peaks are well resolved and scaling due to solvent exchange is not observed for the $^1J_{N3H3}$ coupling constants. The effect of such exchange on the measured $^{3h}J_{H2H3}$ coupling constants could therefore be assumed to be negligible.

The tilt of the E. COSY cross peak also allows the determination of the sign of the $^{3h}J_{H2H3}$ scalar coupling constants. In the $^{2h}J_{NN}$-HNN-E. COSY experiment, the tilt is inverted due to the application of the last non-selective 180° proton pulse during the reverse INEPT period (Figure 2B). This must be taken into account to establish the correct relative sign of the two coupling constants involved. The observed negative tilt in the $^{2h}J_{NN}$-HNN-E. COSY experiment therefore represents a true positive displacement of the E. COSY cross peak components by the passive spin. Since γ_N is negative and γ_H is positive, a positive tilt indicates that the relative sign of the $^{3h}J_{H2H3}$ coupling constant is opposite to that of the $^1J_{N3H3}$ coupling constant. Thus, with the $^1J_{N3H3}$ coupling constant negative, the $^{3h}J_{H2H3}$ coupling constant is positive.

The $^{2h}J_{NN}$-HNN-E. COSY experiment is demonstrated on two uniformly ^{15}N-labeled RNA hairpins (Figure 3), the 29mer CopA29 and the 23mer DIS23-AG. Figure 3 shows the adenosine H2 → uracil N3 correlated regions of the experiment applied to the uniformly ^{15}N labeled CopA29 and DIS23-AG hairpins at 298 K. For the DIS23-AG hairpin, $^{3h}J_{H2H3}$ coupling constants were measured using the H2-N3 correlated cross peaks from two AU base-pairs (U6-A18 and U3-A21) in the stem helix. For the CopA29 hairpin, $^{3h}J_{H2H3}$ coupling constants were measured for four of the five AU base-pairs located in both the upper and lower stem regions (U4-A26, U5-A25, U6-A24 and U12-A19). The $^{3h}J_{H2H3}$ coupling constants measured for six AU base-pairs in the two RNA hairpins was found to range in magnitude from 0.1 to 1.8 Hz with an estimated error based on the signal-to-noise ratio of

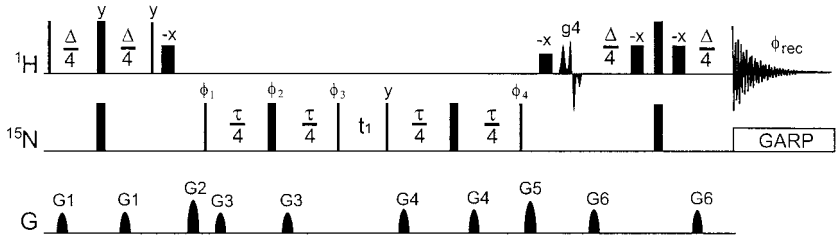

Figure 1. $^{2h}J_{NN}$-HNN-E. COSY pulse sequence for the measurement of $^{3h}J_{H2H3}$ coupling constants based on a modified version of the original $^{2h}J_{NN}$-HNN-COSY experiment with a selective 90° proton pulse used in the back-transfer to the AH2 protons and no proton decoupling during t_1. Narrow and wide rectangular pulses represent 90° and 180° pulses, respectively. All pulses are applied along x unless otherwise indicated. The proton carrier frequency was centered on the H_2O resonance (~4.7 ppm) and the nitrogen frequency centered between the N1/N3 imino and N1/N3 adenosine resonances (190 ppm). The selective G4-proton pulse is applied centered on the H_2O frequency and covers the entire aromatic region (± 3000 Hz) while leaving the imino protons untouched. Water suppression is accomplished by use of water flip-back H_2O pulses (Grzesiek and Bax, 1993) and a WATERGATE (Piotto et al., 1992) sequence in the final reverse INEPT transfer (H_2O selective rectangular pulses were of 1 ms duration and adjusted with small-angle phase shifts to maximize water suppression). Delays: $\Delta = 33.3$ ms, $\tau = 60$ ms. Sine-bell shaped x,y,z pulsed field gradients were applied as follows: $G_1 = 800$ μs, 5 G cm^{-1}; $G_2 = 2.5$ ms, 17 G cm^{-1}; $G_3 = 1$ ms, 8 G cm^{-1}; $G_4 = 1$ ms, 9.4 G cm^{-1}; $G_5 = 1$ ms, 23 G cm^{-1}; $G_6 = 800$ μs, 24 G cm^{-1}. ^{15}N decoupling was achieved using GARP (Shaka et al., 1985) with an effective bandwidth of 7.25 kHz. Phase cycle: ϕ_1 = x, −x; ϕ_2 = x; ϕ_3 = 4(y), 4(−y); ϕ_4 = 2(x), 2(−x); ϕ_5 = 2(x), 2(−x); Rec = (x, −x, −x, x). Quadrature detection in the ω_1 dimension is obtained by incrementing ϕ_1, ϕ_2 and ϕ_3 according to States-TPPI (Marion et al., 1989).

the cross peak, which ranged from ± 0.1 to 0.3 Hz. For the small $^{3h}J_{H2H3}$ coupling constants, the precision of the measurement does not allow the exclusion of the possibility that the value of the coupling constants are actually zero or slightly negative. In fact, the calculations described here predict that the $^{3h}J_{H2H3}$ coupling constant will cross a zero point and become slightly negative as the strength of the H-bond decreases.

An examination of the dependence of the $^{3h}J_{H2H3}$ coupling constant on the position of the AU base-pair within the hairpins reveals an interesting correlation. While relatively strong $^{3h}J_{H2H3}$ coupling constants of 1.6 Hz to 1.8 Hz were measured for the U3-A21 base pair in DIS23-AG and the U4-A26 and U5-A25 base-pairs in CopA29, which are in well-stacked helical regions, smaller $^{3h}J_{H2H3}$ coupling constants of 0.1 to 1.0 Hz are found for the three other AU base pairs located in these hairpins either proximal to or within more dynamic regions of the RNA structure. As previously reported, the U12-A19 base pair of CopA29 is located within a highly dynamic stem region of this RNA hairpin and U6-A18 of DIS-AG and U6-A24 of CopA29 are both only one base pair away from loop and bulge regions, respectively. Thus, the observed differences in the $^{3h}J_{H2H3}$ coupling constants may provide a sensitive probe for correlating base pair stability and dynamics, which other NMR measurements may be unable to detect. For example, the small $^{3h}J_{H2H3}$ coupling constant measured for the U6-A24 base pair in CopA29 may indicate that the geometry or stability of this base pair is affected by the dynamics of the neighboring bulge. Such a perturbation of U6-A24 is not obvious from the line width of the imino proton resonance, its chemical shift, nor the $^{2h}J_{N1N3}$ trans-hydrogen bond coupling constant associated with the base pair, all of which show no significant differences when compared to the U5-A25 and U4-A26 base pairs in the same hairpin. The $^{3h}J_{H2H3}$ coupling constant measurements further suggest that an AU base pair must be at least two base pairs away from a dynamic region or RNA structure (e.g., bulge, loop or junction) for it to be paired and stacked in a stable, unperturbed conformation. This notion is in agreement with previous studies that have systematically tested effects of flanking base pair sequences on the stability of different base pairs within RNA helices (Turner et al., 1988).

It is interesting to note that in the CopA29 hairpin, a small $^{3h}J_{H2H3}$ coupling constant (0.1 Hz) is observed for the U12-A19 base pair, for which the imino proton is unobservable due to exchange broadening. Observable $^{2h}J_{N1N3}$ coupling constants have previously been reported for this base pair as well as the A10-U21 pair, for which an imino proton is also not observed. In the $^{2h}J_{NN}$-HNN-E. COSY experiment, the measured $^{1}J_{H3N3}$ splitting of the A10-U21 base pair associated cross peak shown in Figure 3B is only about 90% of the magnitude observed for the other U4-A26, U5-A25 and U6-A24 base pairs, consistent with the observation of a relatively smaller $^{2h}J_{NN}$ coupling constant of ~5.7 Hz (Luy and Marino, 2000) as well as a reduced $^{3h}J_{H2H3}$ coupling constant.

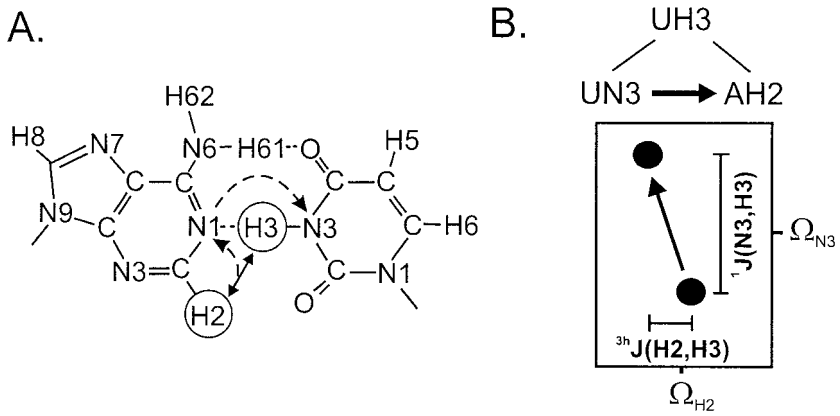

Figure 2. (A) AU base pair scheme with the expected magnetization transfer pathway of the $^{2h}J_{NN}$-HNN-E. COSY experiment indicated by dashed arrows. The $^{3h}J_{H2H3}$ coupled protons are circled and connected by a solid arrow. In the $^{2h}J_{NN}$-HNN-E. COSY experiment, the relatively large $^{1}J_{N3H3}$ coupling constant (−90 Hz) is active during the t_1 evolution period and serves to separate the doublet components of the E. COSY cross peak. The selective G4-pulse leaves the spin-state of H3 unperturbed so that the $^{3h}J_{H2H3}$ coupling can be accurately measured by the displacement of the E. COSY doublet in the directly detected dimension. (B) The expected E. COSY cross peak pattern with the participating atoms and coupling constants. Since a non-selective 180° proton pulse is applied during the back transfer the observed E. COSY tilt is inverted relative to the actual sign of the coupling constant.

From these measurements, a simple model can be derived for the dynamic exchange of states for U12-A19, in which the bases form a standard canonical pair approximately 90% of the time, while 10% of the time very weak or no hydrogen bond-mediated base pairing is found between these nucleotides. Although an E. COSY cross peak correlation was not observed in the $^{2h}J_{NN}$-HNN-E. COSY experiment for the A10-U21 due to a low signal-to-noise ratio, this base pair may also experience a similar dynamic.

To investigate variations in the $^{3h}J_{H2H3}$ coupling constants as a function of hydrogen bond length and geometry, DFT/FPT calculations were performed using a fragment of an AU base pair (Figure 4A) with varied base pair angular geometries and bond distances. A DFT calculation of the absolute value of the $^{3h}J_{H2H3}$ coupling constant with respect to the N1-H3 distance is shown in Figure 4B for a fixed N3-H3 distance of 1.08 Å. The DFT/FPT calculation clearly shows the strong dependence of the magnitude of the $^{3h}J_{H2H3}$ coupling constant on the N1-H3 distance and a predicted $^{3h}J_{H2H3}$ coupling constant of $\sim$0.1 Hz for a canonical AU base pair geometry. In contrast, mimicking propeller twisting by rotation of the base planes with respect to the N1···H3-N3 H-bond over a range of $\phi = -45°$ to 25° resulted in no significant change in the calculated $^{3h}J_{H2H3}$ coupling constant (Figure 5A). By varying the planar angle ζ subtended by the C2-N1 and N1···H3 bond vectors over a range from 100° to 130°, a maximum value for $^{3h}J_{H2H3}$ coupling constants was found between 105° and 110°. This maximal value for the $^{3h}J_{H2H3}$ coupling constant is approximately a factor of 2 larger than observed when $\zeta = 117°$, as is found for ideal AU base pair geometry (Figure 5B). The variation of the dihedral angle θ subtended by the H2-C2 and N1···H3 bond vectors is shown in Figure 5C. Variation of the dihedral angle θ is accomplished in the calculations by varying the H-bond geometry, while leaving the adenosine base geometry fixed. Unlike the relatively significant changes in the strength of the $^{3h}J_{H2H3}$ coupling constant predicted as a result of small changes in ζ, a change in the dihedral angle of 50° is required to increase the magnitude of the $^{3h}J_{H2H3}$ coupling constant two-fold compared to ideal AU base pair geometry where θ is approximately 0°. Although not carried out here due to insufficient data, the dihedral nature of the angle θ lends itself to the possibility of fitting the variation in this coupling constant using an empirically derived Karplus-like equation.

The sign of the $^{3h}J_{H2H3}$ coupling constants predicted by the DFT/FPT calculations is positive and matches well with experimental data. In general, however, the absolute values of the $^{3h}J_{H2H3}$ coupling constants calculated by the DFT/FPT calculations are smaller than the experimental observed coupling constants. The latter result was unexpected since previous studies have shown that such calculations could reproduce the magnitude and sign of measured trans-hydrogen bond HN and NN coupling constants fairly

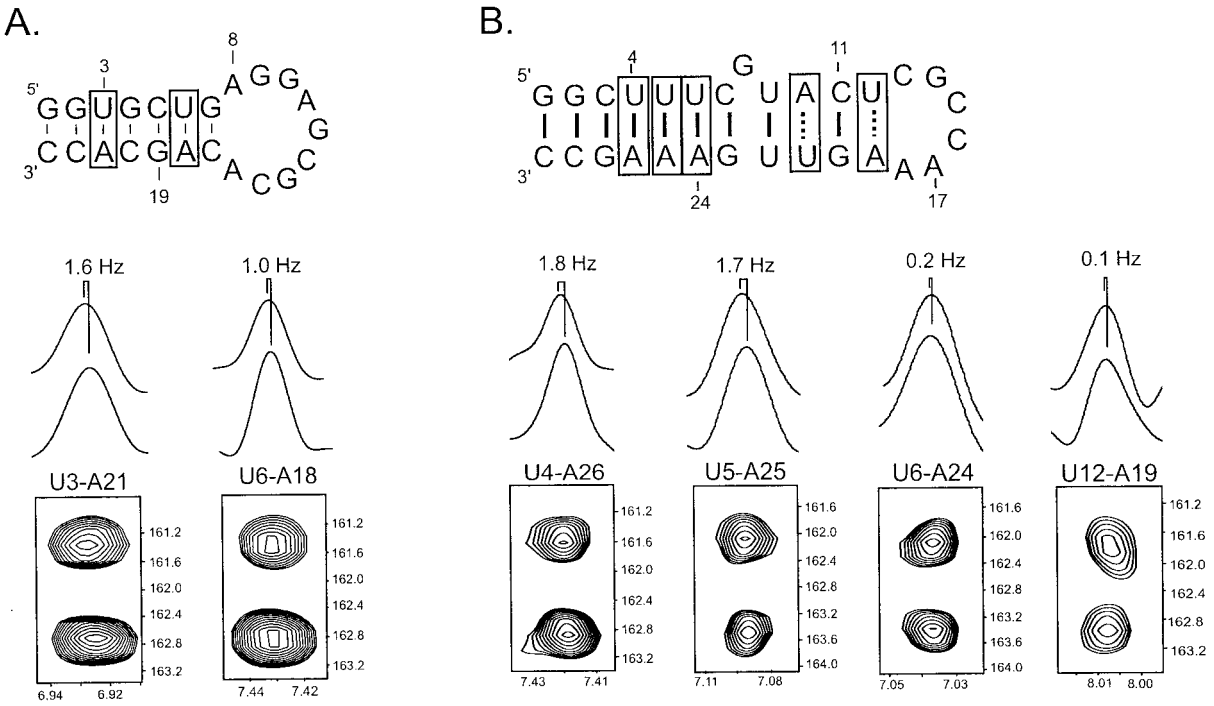

Figure 3. (A) Schematic of the nucleotide-sequence and secondary structure of the RNA hairpin DIS23-AG used to demonstrate the $^{2h}J_{NN}$-HNN-E. COSY experiment. AU base pairs in the stem region of the hairpin are boxed. The pulse sequence was applied to a ~ 1.5 mM DIS23-AG sample using 128 and 2048 complex points in t_1 and t_2, respectively, and 256 scans per increment to maximize the experimental signal to noise ratio. The E. COSY cross peaks measured for base pairs U6-A18 and U3-A21 in DIS23-AG, along with appropriate 1D F_2 traces through the center of the peaks, are shown and labeled with the determined $^{3h}J_{H2H3}$ coupling constant. The coupling constants could be measured with an estimated accuracy of about ± 0.1 Hz based on the signal-to-noise of the spectrum. (B) Nucleotide sequence and secondary structure of the RNA hairpin CopA29. AU base pairs in the stem region of the hairpin are boxed with the three observed canonical AU base pairs connected with solid lines and the two AU base pairs observed to have strongly exchange-broadened imino protons connected by dashed lines. The $^{2h}J_{NN}$-HNN-E. COSY experiment was applied to this RNA hairpin using the identical parameters as for DIS23-AG. For the ~ 1 mM CopA29 sample this lead to a signal-to-noise ratio that gave an estimated error of ± 0.15 Hz for the measurement of the $^{3h}J_{H2H3}$ displacement in the U5-A26, U6-A25 and U4-A27 base pairs and ± 0.3 Hz for the U12-A19 base pair. The E. COSY cross peaks measured for base pairs U4-A26, U5-A25, U6-A24 and U12-A19 in CopA29), along with appropriate 1D F_2 traces through the center of the peaks, are shown and labeled with the determined $^{3h}J_{H2H3}$ coupling constants. The cross peak associated with U21-A9 could be seen, however the error due to the low signal-to-noise ratio for this exchange-broadened signal was of the order of the measured E. COSY displacement and therefore could not be used to determine a $^{3h}J_{H2H3}$ coupling constant.

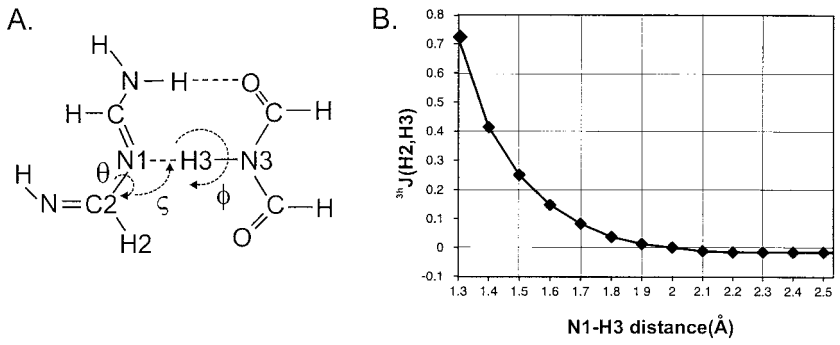

Figure 4. (A) Diagram of the AU fragment used to simulate the dependence of the $^{3h}J_{H2H3}$ couplings on the N1···H3-N3 hydrogen bond length and differences in base pair geometry. The angular variations for which the $^{3h}J_{H2H3}$ coupling constant was calculated are shown: A rotation of the bases relative to each other equivalent to a propeller twist is defined by the angle ϕ, the planar angle ζ, associated with the bond vectors C2-N1 and N1···H3, defines a geometrical change that is similar to an opening or closing of the base pair and a rotation about the dihedral angle θ, subtended by the bond vectors H2-C2 and N1···H3 is similar to a base pair buckle. (B) Plot of the dependence of the magnitude of the $^{3h}J_{H2H3}$ coupling constant on the N1-H3 hydrogen bonding distance.

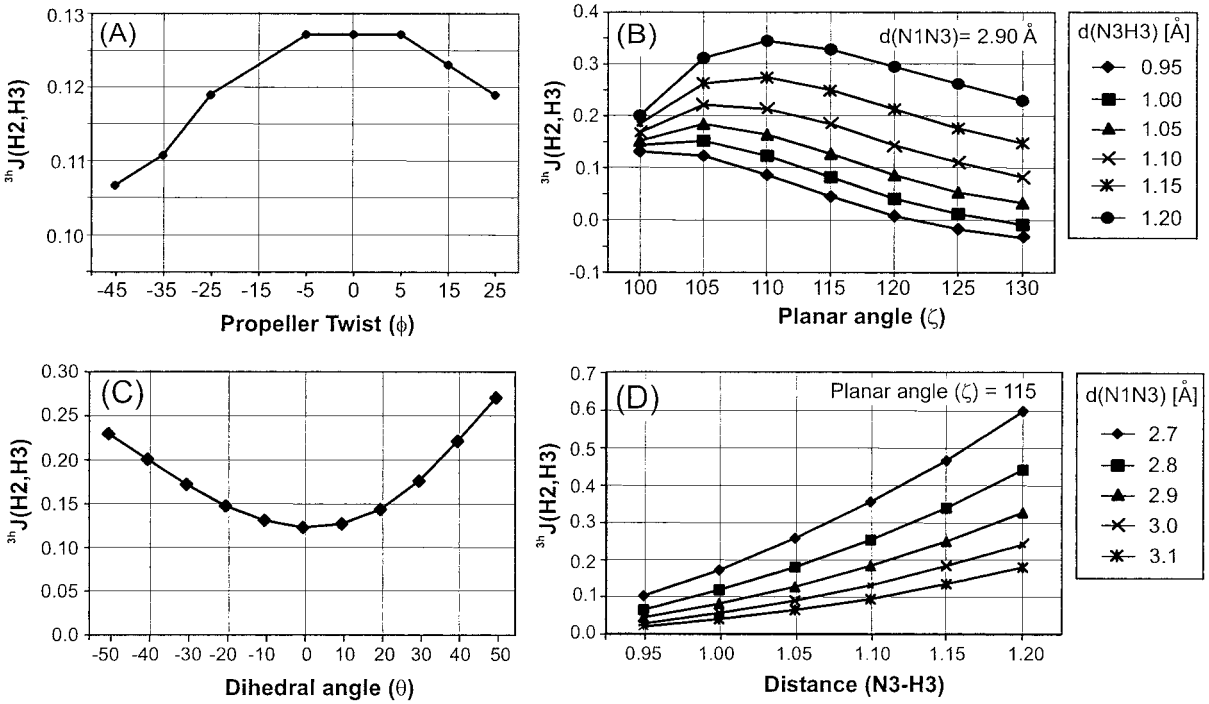

Figure 5. (A) Plot of the dependence of the magnitude of the $^{3h}J_{H2H3}$ coupling constant on the propeller twist, ϕ, with respect to the N1···H3-N3 axis. (B) Plot of the dependence of the magnitude of the $^{3h}J_{H2H3}$ coupling constant on the planar angle ζ spanned by the atoms C2-N1···H3. The maximum value for the $^{3h}J_{H2H3}$ coupling constant is found for an angle between 105° and 110°, which is smaller than the angle found for the idealized geometry of an AU base pair, which is ∼ 117°. The calculations are shown for different H3-N3 distances ranging from 0.95 to 1.2 Å (individual traces are identified by the accompanying box). (C) Plot of the dependence of the magnitude of the $^{3h}J_{H2H3}$ on the dihedral angle, θ defined by the atomic vectors H2-C2 and N1···H3. A Karplus-like dependence is observed for the variation of this angle with respect to the magnitude of the $^{3h}J_{H2H3}$ coupling constant; however, the predicted variation within the physical limits for the angle in normal RNA structure is quite small. (D) Plot of the dependence of the magnitude of the $^{3h}J_{H2H3}$ coupling constant on the H3-N3 distance, using N1-N3 distances ranging from 2.7 to 3.1 Å (individual traces are identified by the accompanying box).

well (Barfield et al., 2001; Dingley et al., 1999; Scheurer and Bruschweiler, 1999) and may indicate a limitation in the current DFT/FPT method for predicting trans-hydrogen bond HH couplings. The inclusion of additional terms besides the Fermi contact values, such as the paramagnetic spin-orbit and diamagnetic spin-orbit contributions, may be required to yield more accurate calculations of the $^{3h}J_{H2H3}$ coupling constants. Nonetheless, the relative trends in the magnitude in response to changes in H-bond distance and geometry can be used to make qualitative comparisons with experimentally observed coupling constants. For example, although the angular dependence of the $^{3h}J_{H2H3}$ coupling constant is predicted to be small, the DFT/FPT calculations indicate that relatively large changes in the size of the coupling constants are expected as a result of variation in the H-bond distance, which correlates well with the experimentally observed attenuation of $^{3h}J_{H2H3}$ coupling constants for dynamic base pairs in this study. The DFT/FPT calculations show an exponential relationship between the $^{3h}J_{H2H3}$ coupling constant and the N1-H3 bond distance (Figure 4B), suggesting that these coupling constants should be a sensitive measure of the strength of hydrogen bonds. Additional calculations show that shorter N1-N3 and longer N3-H3 distances should also correlate with larger $^{3h}J_{H2H3}$ coupling constants. An example of results of these calculations for a fixed planar angle of 115° is shown in Figure 5D. Calculations of the effect of varied N1-N3 and N3-H3 distances on the $^{3h}J_{H2H3}$ coupling constants were also carried out using other propeller twist angles ranging from 100° to 130° (data not shown). In these calculations, the overall trend in magnitude of the $^{3h}J_{H2H3}$ coupling constant was the same as observed in Figure 5D; that is, the $^{3h}J_{H2H3}$ coupling constants become larger as the H3-N3 distance increases and the H3-N1 and N1-N3 distances decrease. A sim-

ilar trend has also been observed for the relationship between N1-N3 and N3-H3 distances and the magnitude of $^{2h}J_{NN}$ and $^{1h}J_{HN}$ coupling constants across base pair H-bonds (Dingley et al., 1999; Barfield et al., 2001). However, over the range of N1-N3 distances simulated here, the $^{2h}J_{NN}$ coupling constants are predicted to vary by only approximately two-fold, while the $^{3h}J_{H2H3}$ coupling constants are predicted to vary by approximately six-fold. The $^{3h}J_{H2H3}$ coupling constants may therefore be more sensitive to small changes in H-bond strength that may result from either a dynamic or static reduction of only a few tenths of an Ångström in the H-bond distance.

In contrast, major angular distortions of the geometry of the base pair are predicted to be required to significantly change the magnitude of $^{3h}J_{H2H3}$ coupling constants and are therefore unlikely to be the source of large variation in the size of observed coupling constants. Nevertheless, a rigorous deconvolution of the dependency of the $^{3h}J_{H2H3}$ coupling constant on H-bond angular geometry versus distances will be necessary for an unambiguous analysis of these coupling constants and this will require high-resolution structures for the CopA29 and DIS23-AG RNA hairpins from which structural parameters can be independently derived. Such structures are unavailable at this time.

Conclusion

The measurement of $^{3h}J_{H2H3}$ coupling constants provides a new probe for identifying differences in local AU base pair geometry and dynamics in RNA oligonucleotides. From the RNA hairpins measured in this study, $^{3h}J_{H2H3}$ coupling constants in the range of 1.6–1.8 Hz appear to correlate with relatively strong H-bonds associated with AU base pairs in unperturbed, well stacked helical environments; while, smaller coupling constants in the range of 0.1 to 1.0 Hz appear to correlate with weaker H-bonds and potentially larger amplitude motions of the base pair. DFT/FPT calculations corroborate the observations, predicting the relative sign and observed trends in magnitude of the coupling constants. Further analysis, however, is still required to understand the difference between the observed and calculated magnitudes for the $^{3h}J_{H2H3}$ coupling constants and to allow a more refined analysis of the contributions of base pair angular geometry versus H-bond distances on the size of $^{3h}J_{H2H3}$ coupling constants. Nevertheless, structural and dynamic information derived from the measurement of $^{3h}J_{H2H3}$ coupling constants can now be used qualitatively in conjunction with other measures of H-bond strength, to gain a better understanding of the strength of interatomic interactions in RNA folds and complexes.

Acknowledgements

This work was supported by an NIH grant (GM 59107-01) to J.P.M. B.L. acknowledges a Feodor-Lynen fellowship, E.S. DeJong is an NRC postdoctoral fellow and U. Richter a NIST visiting foreign fellow. We thank F. Song for oligonucleotide synthesis and M. Barfield (University of Arizona) for helpful discussions and sharing unpublished data.

References

Arnold, W.D. and Oldfield, E. (2000) *J. Am. Chem. Soc.*, **122**, 12835–12841.

Barfield, M. (2002) *J. Am. Chem. Soc.*, **124**, 4158–4168.

Barfield, M., Dingley, A.J., Feigon, J. and Grzesiek, S. (2001) *J. Am. Chem. Soc.*, **123**, 4014–4022.

Batey, R.T., Inada, M., Kujawinski, E., Puglisi, J.D. and Williamson, J.R. (1992) *Nucl. Acids Res.*, **20**, 4515–4523.

Benedict, H., Shenderovich, I.G., Malkina, O.L., Malkin, V.G., Denisov, G.S., Golubev, N.S. and Limbach, H.H. (2000) *J. Am. Chem. Soc.*, **122**, 1979–1988.

Bryce, D.L. and Wasylishen, R.E. (2001) *J. Biomol. NMR*, **19**, 371–375.

Cordier, F. and Grzesiek, S. (1999) *J. Am. Chem. Soc.*, **121**, 1601–1602.

Cordier, F., Rogowski, M., Grzesiek, S. and Bax, A. (1999) *J. Magn. Reson.*, **140**, 510–512.

Cornilescu, G., Hu, J.S. and Bax, A. (1999a) *J. Am. Chem. Soc.*, **121**, 2949–2950.

Cornilescu, G., Ramirez, B.E., Frank, M.K., Clore, G.M., Gronenborn, A.M. and Bax, A. (1999b) *J. Am. Chem. Soc.*, **121**, 6275–6279.

Czernek, J. and Bruschweiler, R. (2001) *J. Am. Chem. Soc.*, **123**, 11079–11080.

Czernek, J., Fiala, R. and Sklenar, V. (2000) *J. Magn. Reson.*, **145**, 142–146.

Del Bene, J.E. and Bartlett, R.J. (2000) *J. Am. Chem. Soc.*, **122**, 10480–10481.

Del Bene, J.E. and Jordan, M.J.T. (2001) *J. Mol. Struct. Theochem.*, **573**, 11–23.

Del Bene, J.E., Perera, S.A. and Bartlett, R.J. (2001) *Magn. Reson. Chem.*, **39**, S109–S114.

Dingley, A.J. and Grzesiek, S. (1998) *J. Am. Chem. Soc.*, **120**, 8293–8297.

Dingley, A.J., Cordier, F. and Grzesiek, S. (2001) *Conc. Magn. Reson.*, **13**, 103–127.

Dingley, A.J., Masse, J.E., Peterson, R.D., Barfield, M., Feigon, J. and Grzesiek, S. (1999) *J. Am. Chem. Soc.*, **121**, 6019–6027.

Dingley, A.J., Masse, J.E., Feigon, J. and Grzesiek, S. (2000) *J. Biomol. NMR*, **16**, 279–289.

Dunger, A., Limbach, H.H. and Weisz, K. (2000) *J. Am. Chem. Soc.*, **122**, 10109–10114.
Emsley, L. and Bodenhausen, G. (1989) *J. Magn. Reson.*, **82**, 211–221.
Geertsen, J., Odderschede, J., Scuseria, G.J. (1987) *Chem. Phys.*, **87**, 2138.
Gemmecker, G. (2000) *Angew. Chem.*, **112**, 1276–1279; *Int. Ed.*, **39**, 1224–1226.
Griesinger, C., Sørensen, O.W. and Ernst, R.R. (1985) *J. Am. Chem. Soc.*, **107**, 6394–6396.
Griesinger, C., Sørensen, O.W. and Ernst, R.R. (1986) *J. Chem. Phys.*, **85**, 6837–6852.
Griesinger, C., Sørensen, O.W. and Ernst, R.R. (1987) *J. Magn. Reson.*, **75**, 474–492.
Grzesiek, S. and Bax, A. (1993) *J. Biomol. NMR*, **3**, 627–638.
Grzesiek, S., Cordier, F. and Dingley, A.J. (2001) *Meth. Enzymol.*, **338**, 111–133.
Guerra, C.F., Bickelhaupt, F.M., Snijders, J.G. and Baerends, E.J. (2000) *J. Am. Chem. Soc.*, **122**, 4117–4128.
Hennig, M. and Geierstanger, B.H. (1999) *J. Am. Chem. Soc.*, **121**, 5123–5126.
Hennig, M. and Williamson, J.R. (2000) *Nucl. Acids Res.*, **28**, 1585–1593.
Liu, A.Z., Hu, W.D., Majumdar, A., Rosen, M.K. and Patel, D.J. (2000) *J. Biomol. NMR*, **17**, 305–310.
Liu, A.Z., Majumdar, A., Hu, W.D., Kettani, A., Skripkin, E. and Patel, D.J. (2000) *J. Am. Chem. Soc.*, **122**, 3206–3210.
Lohr, F., Mayhew, S.G. and Rüterjans, H. (2000) *J. Am. Chem. Soc.*, **122**, 9289–9295.
Luy, B. and Marino, J.P. (2000) *J. Am. Chem. Soc.*, **122**, 8095–8096.
Majumdar, A. (2001) *Magn. Reson. Chem.*, **39**, S166–S170.
Majumdar, A. and Patel, D.J. (2002) *Acc. Chem. Res.*, **35**, 1–11.
Majumdar, A., Gosser, Y. and Patel, D.J. (2001a) *J. Biomol. NMR*, **21**, 289–306.
Majumdar, A., Kettani, A., Skripkin, E. and Patel, D.J. (2001b) *J. Biomol. NMR*, **19**, 103–113.
Majumdar, A., Kettani, A. and Skripkin, E. (1999a) *J. Biomol. NMR*, **14**, 67–70.
Majumdar, A., Kettani, A., Skripkin, E. and Patel, D. (1999b) *J. Biomol. NMR*, **15**, 207–211.
Malkin, V.G., Malkina, O.L. and Salahub, V.G. (1994) *Chem Phys. Lett.*, **221**, 91–99.
Malkina, O.L., Salahub, D.R. and Malkin, V.G. (1996) *J. Chem. Phys.*, **105**, 8793–8800.
Marion, D., Ikura, R., Tschudin, R. and Bax, A. (1989) *J. Magn. Reson.*, **85**, 393.
Meissner, A. and Sørensen, O.W. (2000a) *J. Magn. Reson.*, **143**, 387–390.
Meissner, A. and Sørensen, O.W. (2000b) *J. Magn. Reson.*, **143**, 431–434.
Milligan, J.F. and Uhlenbeck, O.C. (1989) *Meth. Enzymol.*, **180**, 51.
Mishima, M., Hatanaka, M., Yokoyama, S., Ikegami, T., Wälchli, M., Ito, Y. and Shirakawa, M. (2000) *J. Am. Chem. Soc.*, **122**, 5883–5884.
Nikonowicz, E.P., Sirr, A., Legault, P., Jucker, F.M., Baer, L.M. and Pardi, A. (1992) *Nucl. Acids Res.*, **20**, 4507–4513.
Onak, T., Jaballas, J. and Barfield, M. (1999) *J. Am. Chem. Soc.*, **121**, 2850–2856.
Paillart, J.C., Marquet, R., Skripkin, E., Ehresmann, C. and Ehresmann, B. (1996) *Biochimie*, **78**, 639–653.
Pecul, M., Leszczynski, J. and Sadlej, J. (2000) *J. Phys. Chem. A*, **104**, 8105–8113.
Pervushin, K., Fernandez, C., Riek, R., Ono, A., Kainosho, M. and Wüthrich, K. (2000) *J. Biomol. NMR*, **16**, 39–46.
Pervushin, K., Ono, A., Fernandez, C., Szyperski, T., Kainosho, M. and Wüthrich, K. (1998) *Proc. Natl. Acad. Sci. USA*, **95**, 14147–14151.
Pietrzak, M., Wehling, J., Limbach, H.H., Golubev, N.S., Lopez, C., Claramunt, R.M. and Elguero, J. (2001) *J. Am. Chem. Soc.*, **123**, 4338–4339.
Piotto, M., Saudek, V. and Sklenar, V. (1992) *J. Biomol. NMR*, **2**, 661–665.
Pople, J.A., McIver, Jr. J.W. and Ostlund, N.S. (1968) *J. Chem. Phys.* **49**, 2960–2964, 2965–2970.
Schaftenaar, G. and Noordik, J.H. (2000) *J. Comput.-Aided Mol. Des.*, **14**, 123–134.
Scheurer, C. and Bruschweiler, R. (1999) *J. Am. Chem. Soc.*, **121**, 8661–8662.
Shaka, A.J., Barker, P. and Freeman, R.J. (1985) *J. Magn. Reson.*, **64**, 547–552.
Turner, D.H., Sugimoto, N. and Freier, S.M. (1988) *Annu. Rev. Biophys. Chem.*, **17**, 167–192.
Wagner, E.G.H. and Simons, R.W. (1994) *Annu. Rev. Microbiol.*, **48**, 712–742.
Wang, Y.X., Jacob, J., Cordier, F., Wingfield, P., Stahl, S.J., Lee-Huang, S., Torchia, D., Grzesiek, S. and Bax, A. (1999) *J. Biomol. NMR*, **14**, 181–184.
Wilkens, S.J., Westler, W.M., Weinhold, F. and Markley, J.L. (2002) *J. Am. Chem. Soc.*, **124**, 1190–1191.
Wohnert, J., Dingley, A.J., Stoldt, M., Gorlach, M., Grzesiek, S. and Brown, L.R. (1999) *Nucl. Acids Res.*, **27**, 3104–3110.